Assuming complete filling of the layers ($\zeta \leq 1$), then $m/n = \sigma$, and

$$\Xi^{1/n} = (\sigma)^{-\sigma}\frac{a^{1-\sigma}}{(2\pi)^{1/2n}} \qquad (A.3)$$

Upon taking the logarithm, we obtain the configurational free energy, F:

$$\frac{F}{nkT} \simeq \sigma \ln(\sigma) - (1-\sigma)\ln(a) + \frac{1}{2n}\ln(2\pi) \qquad (A.4)$$

and thus, relative to the crystal ($\sigma = 1$)

$$\frac{\Delta F}{nkT} = \frac{F - F(\sigma = 1)}{nkT} = \sigma \ln(\sigma) - (1-\sigma)\ln(a) \qquad (A.5)$$

References and Notes

(1) Dill, K. A. "Surfactants in Solution"; Mittal, K. L., Lindman, B., Eds.; Plenum Press: in press.
(2) Dill, K. A.; Flory, P. J. *Proc. Natl. Acad. Sci. U.S.A.* **1980**, *77*, 3115.
(3) Dill, K. A.; Flory, P. J. *Proc. Natl. Acad. Sci. U.S.A.* **1981**, *78*, 676.
(4) Seelig, J.; Seelig, A. *Q. Rev. Biophys.* **1980**, *13*, 19.
(5) Dill, K. A. *J. Phys. Chem.* **1982**, *86*, 1498.
(6) Cantor, R. S.; Dill, K. A. *Macromolecules*, following paper in this issue.

Statistical Thermodynamics of Short-Chain Molecule Interphases. 2. Configurational Properties of Amphiphilic Aggregates

Robert S. Cantor* and Ken A. Dill

Department of Pharmaceutical Chemistry, School of Pharmacy, University of California, San Francisco, California 94143.

Received May 9, 1983

ABSTRACT: In the preceding paper, formal expressions for configurational properties of short-chain molecule interphases have been derived. In the present work, expressions giving positional and orientational probability distributions of chain segments and bonds are evaluated for the case of planar systems (representing monolayers at an oil/water interface or bilayers). Configurational properties (e.g., order parameter, chain segment distributions, and probabilities of chain bends) are evaluated as a function of bending energy, length, and surface density of the chains. Results of neutron diffraction experiments on widths of segment position distributions are compared to predictions of the model and are found to be in good agreement. Calculated chain-averaged properties (order parameter and bends/chain averaged over the interphase) are presented as functions of area/chain and are found to fit simple exponential functions remarkably well. For planar systems, chain stiffness is predicted to have relatively little effect on configurational properties, which are determined largely by intermolecular constraints.

In the preceding article,[1] we presented a statistical mechanical formalism which may be used to predict structural and thermodynamic properties of the hydrocarbon regions of amphiphilic chain molecule interphases such as surfactant monolayers, bilayers, and micelles. The lattice model presented therein provides a framework to account for the distribution of the chain configurations in terms, primarily, of three variables: the surface density of the chains relative to that of the crystal (σ), the number, $n + 1$, of flexible segments along the chains, and the energy ϵ, required to convert a bond pair which is collinear to that which is bent at a right angle. Calculations presented here demonstrate the effect which varying these parameters is predicted to have on structural properties such as the distribution of the chain ends, measurable through neutron scattering experiments, and on the order parameter, measurable by NMR methods. The prediction of thermal properties will be described in forthcoming work.

In this work we consider only planar aggregates: monolayers at an oil/water interface or bilayers wherein the area available to the chains is constant with depth. For representative calculations from the model, we have arbitrarily chosen a standard case, for which, in the terminology of the preceding paper,[1] the coordination number of the simple cubic lattice is $z = 6$ and chains have $n + 1 = 11$ segments, are freely flexible ($\epsilon = \epsilon_h = 0$; $\omega = \omega_h = 1$), and have approximately the surface density of dipalmitoyllecithin bilayers at their melt temperature (i.e., $\sigma = 0.64$[4]). Since for n-alkyl chains, each lattice segment represents approximately 3.6 methylene groups along the chain,[1] this standard case corresponds to chains with approximately 40 CH_2 groups. This chain length was chosen to allow reasonable resolution in graphic representations of those properties which depend on depth within the interphase (layer number) or position along the chain (segment or bond number). However, for the purpose of comparison with experimental data, calculations are also performed for systems having chains of shorter length.

1. Properties Which Depend on Distance from the Interface

Chain segments are distributed at various depths within the interphase. The depths are represented as discrete layers in the lattice model.[1] The distribution of the probability of occurrence of a given segment throughout these layers (eq 3.5, ref 1), is shown in Figure 1 for the standard case specified above. Data are presented for three representative segments: one near the head group, one in the middle, and one at the end of the chain. Segments nearer the head group along the chain are predicted to occur in layers nearer the interface and are distributed less broadly along the axis normal to the interface than those nearer the chain ends. This point is made more clearly in Figure 2, which shows a measure of the width of the distribution of each chain segment. The width, δ, is the square root of the second moment of the distribution and is given in units of lattice layers. In Figure 2 (and Figure 3, in which the complete distribution is shown for terminal segments only) three curves are given representing different chain stiffnesses: $\omega = \omega_h = 1, 0.5, 0.2$, corresponding to bending energies $\epsilon = \epsilon_h = 0, 0.69kT$, and $1.61kT$, respectively. Stiffer chains are predicted to have broader segment distributions; this effect is most pronounced near chain ends.

0024-9297/84/2217-0384$01.50/0

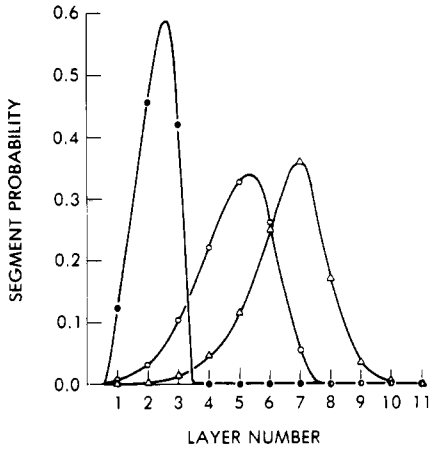

Figure 1. Predicted distributions of chain segments 3 (●), 7 (○), and 11 (△) from the polar headgroup as a function of distance from the interface. For the standard case defined in the text: $n = 10$, $\sigma = 0.64$, and $\omega = \omega_h = 1$. Curves are normalized to an area of 1. For Figures 1–9, the points are results of calculations according to the theory and are connected by a continuous line.

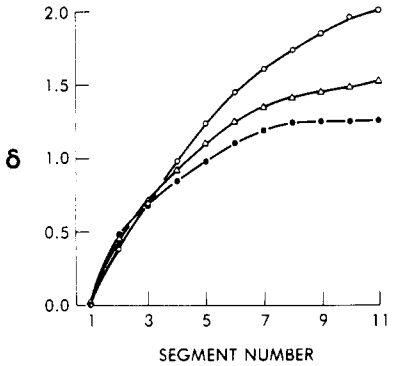

Figure 2. Calculated width, δ, of the segment probability distributions for $n = 10$ and $\sigma = 0.64$ vs. position along the chain (segment number) for chains of varying stiffness: $\omega = 1$ (●), $\omega = 0.5$ (△), and $\omega = 0.2$ (○), with $\omega = \omega_h$ in all cases.

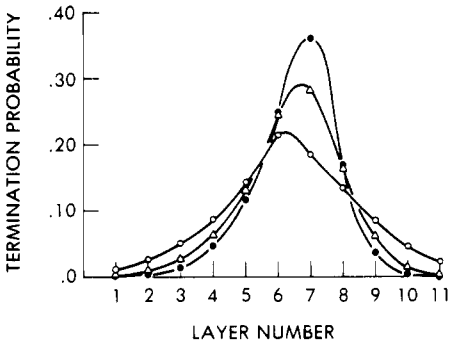

Figure 3. Calculated spatial probability distribution of the terminal chain segment ($n = 10$, $\sigma = 0.64$) for systems with chains of different stiffness, $\omega = 1.0$ (●), $\omega = 0.5$ (△), and $\omega = 0.2$ (○), with $\omega = \omega_h$.

These theoretical predictions are compared to results of neutron diffraction experiments in Figure 4. The experiments have been performed on selectively deuterated dipalmitoyllecithin bilayer membranes in the L_α phase by Zaccai et al.[2] They have measured the half-widths, ν, at $1/e$ height of the distributions of the 4th, 9th, and 12th methylene carbons from the head groups. The experimental system most closely corresponds to representation in the lattice model by chains having $n + 1 = 5$ segments and $\sigma = 0.64$. Calculations are presented for this case in Figure 4, for several values of the chain bending energy ϵ, corresponding to $\omega = \omega_h = 1.0$, 0.5, 0.3, and 0.2. The width in angstroms is given by 4.5δ, since each lattice layer

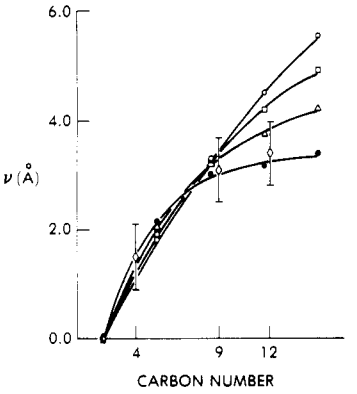

Figure 4. Comparison of calculated and experimentally obtained widths of spatial distributions of chain segments. Results of neutron diffraction experiments of Zaccai et al.[2] on dipalmitoyllecithin bilayers in the L_α phase are given for segments 4, 9, and 12 (◇). Calculated results ($n = 4$, $\sigma = 0.64$) are shown for chains of different stiffness: $\omega = 1.0$ (●), 0.5 (△), 0.3 (□), and 0.2 (○).

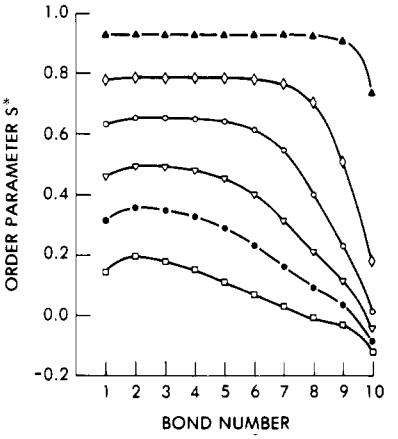

Figure 5. Predicted dependence of order parameter S^* on position along the chain (bond number) for systems of $n = 10$, $\omega = \omega_h = 1$, for different values of chain surface density σ: $\sigma = 0.95$ (▲), 0.85 (◇), 0.75 (○), 0.64 (▽), 0.55 (●), and 0.45 (□).

represents a region of space approximately 4.5 Å wide.[3] Second moments computed in this way are not identical with half-widths at $1/e$ height. If the distributions were Gaussian, for example, these two measures of distribution widths would differ by approximately 12%. Since the distributions are not predicted to be Gaussian, agreement between theory and experiment should be taken as semiquantitative. It appears that insofar as the distribution widths are concerned, lecithin chains are best modeled by ω in the range $0.3 \leq \omega = \omega_h \leq 1.0$. These experiments support the view that the chains in the L_α phase bilayer have configurations which are stochastically distributed,[4] in contrast to the view that chains are collectively tilted.[5]

2. Properties Which Depend on Segment Position and Orientation along the Chains

To avoid contact with solvent, the hydrocarbon chains have a net orientational alignment along an axis normal to the interface. ^{2}H-NMR has been widely used in conjunction with specific deuteration of the methylene groups[6-9] to measure a parameter $S^* = {}^3/_2\langle\cos^2\theta\rangle - {}^1/_2$, characterizing this orientational order, θ being the angle between the chain axis and the interfacial normal and the angular brackets denoting the configurational average.

The statistical mechanical lattice theory permits prediction of S^* (eq 3.6 and 3.15 of ref 1). S^* for each "bond" (two adjacent segments along the lattice chain) is given in Figure 5 for various surface densities. These predictions

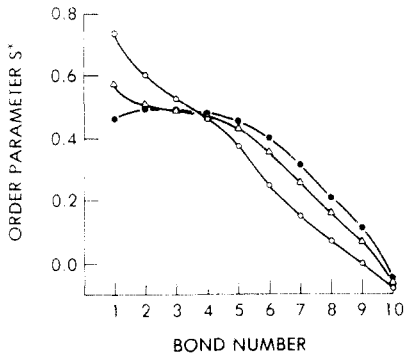

Figure 6. Effect of chain stiffness on the dependence of S^* on position along the chain for systems of $n = 10$, $\sigma = 0.64$, $\omega = \omega_h$, with $\omega = 1.0$ (●), 0.5 (△), and 0.2 (○).

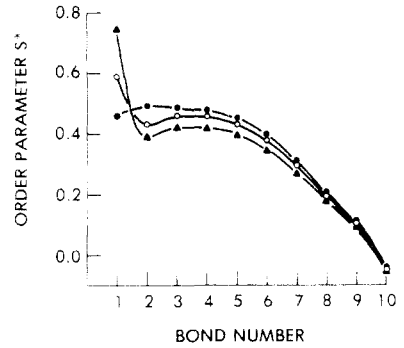

Figure 7. Predicted effect of stiffness of headgroup–chain bond (ω_h) on the order parameter. Data are presented for $\omega_h = 1.0$ (●), 0.4 (○), and 0.1 (▲); in all cases $n = 10$, $\sigma = 0.64$, and $\omega = 1.0$.

do not deviate significantly from those of a simpler interphase model (see Figure 3c of ref 4). According to both treatments, the gradient of decreasing order, and thus of increasing configurational freedom, with depth within the interphase, is a consequence of the reduction in severity of the intermolecular steric constraints brought about by the terminations of some fraction of the chains in each spatial layer. Since segments toward the chain ends tend to be situated deeper within the interphase than segments near the head groups (see Figure 1), the dependence of S^* on position along the chain is similar to the dependence of S on depth within the interphase.

For the planar systems of interest here, chain organization is much more strongly influenced by the steric constraints than by intramolecular forces between adjacent segments along each chain. Shown in Figure 6 is the dependence of S^* on chain stiffness ($\omega = \omega_h = 1.0, 0.5, 0.2$) for $\sigma = 0.64$. The effects are relatively minor compared to those of steric constraints shown in Figure 5. Increased stiffness is predicted to increase the orientational order near the head groups and decrease it toward the chain ends.

For calculations presented in Figures 1–6, it has been assumed that all bond pairs along the chain have the same bending energy. However, the statistical mechanical lattice theory[1] allows for the more general situation that the bond connecting the head group to the first chain segment, the "zeroth" bond, may be chemically different from other bonds along the chain. If the bond pair consisting of the zeroth and first bonds is bent, the statistical weight reduction factor for the first bond, ω_h, may differ from ω. (Since the zeroth bond is assumed always to be forward, this reduction factor is included only for lateral first bonds.) Figure 7 shows the effect of variation of ω_h; all other variables take on the values of the standard case.

The smaller the value of ω_h, the higher the average alignment of the first bond with the interfacial normal.

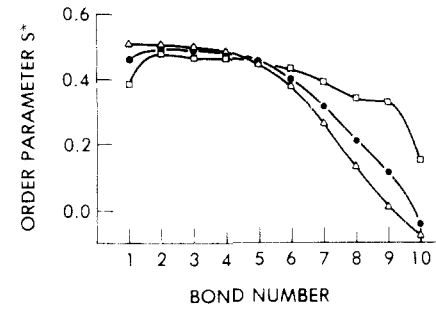

Figure 8. Effect of two lattice parameters on S^*: (●) the standard case, $n = 10$, $\sigma = 0.64$, $\omega = \omega_h = 1$, $z = 6$ ($\beta = \gamma - 1$, no lateral backtracking); (△) the standard case with lateral backtracking allowed ($\beta = \alpha$, see text); (□) $z = 4$, corresponding to a two-dimensional simple cubic lattice; other values are as in the standard case.

Because of the requirement that the first spatial layer be filled, fewer lateral first bonds resulting from increased stiffness of the headgroup–chain connection implies more lateral subsequent bonds in this layer, the consequence of which is slight reduction of the order parameter for all but the first bond. Since the orientation of a given bond depends on the orientation of the two adjacent neighbors along the chain, the behavior of the first and last bonds is qualitatively different from that of internal bonds. This difference arises from the last bond having only one adjacent bond and the first bond being preceded by the "zeroth" bond, which is assumed always to have forward orientation. To assess the importance of this "conditional" nature of bond probabilities, we tested the model as follows. By setting $\alpha = \beta$ in the theory,[1] lateral steps may retrace direction, with the consequence that some lateral bonds may superimpose on their predecessors. Although unphysical, this has the effect of allowing bond orientations to be independent of those of neighboring bonds, for $\omega = 1$. The result is shown in Figure 8: both chain ends have slightly higher order (S^*) when this volume is excluded. The order parameter is thus little dependent on the conditionality of the bond configurations. Also in Figure 8, the standard case for the simple cubic lattice in three dimensions ($z = 6$) is compared to the simple cubic lattice model in two dimensions ($z = 4$). It is clear that the order along the chain is not dissipated as effectively in two-dimensional space where excluded volume constraints are more severe than in three-dimensional systems.

3. Bond-Pair Properties

In the preceding section, we considered the configurations of individual bonds; here we consider the orientations of pairs of adjacent bonds. There are two relative orientations of bond pairs, collinear and bent at 90°, and four absolute orientations (Figure 1 of ref 1), depending on whether each of the two bonds has forward (F) or lateral (L) orientation; bond-pair orientations are denoted FF, FL, LF, and LL. All of the FF pairs are collinear, and all of the FL and LF pairs are bent, but LL pairs may be either collinear or bent. Expressions for the probabilities of the absolute and relative orientations of bond pairs are given in eq 3.16 and 3.17 of ref 1, respectively. Equations 3.16[1] are evaluated for the standard case and plotted in Figure 9a as functions of bond-pair position along the chain. Not surprisingly, the probability of LL pairs increases toward the chain ends, principally at the expense of FF pairs. Figure 9b gives the probability that a pair is bent (eq 3.17 of ref 1) for a range of chain bending energies as a function of position along the chain. As bending energy increases, the probability that a pair is bent is predicted to decrease. The incidence of bends increases toward the chain ends

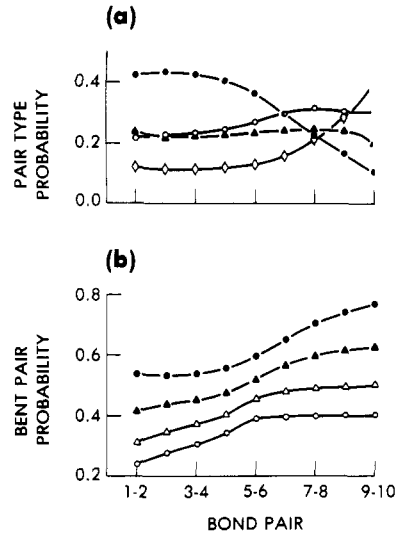

Figure 9. (a) Predicted probability distributions of the four absolute configurations of bond pairs, LL (◊), LF (▲), FL (○), and FF (●), as functions of position along the chain (bond pair number) for the standard case. (b) Probability distribution of a bend bond pair is given for $n = 10$, $\sigma = 0.64$, and $\omega = \omega_h$ for varying chain stiffness: $\omega = 1.0$ (●), 0.5 (▲), 0.3 (△), and 0.2 (○).

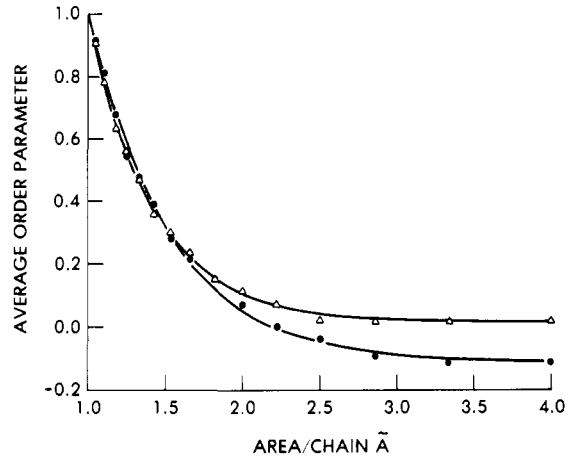

Figure 10. Lattice model predictions of the average order parameter $\bar{S}$ as a function of reduced area/chain, $\tilde{A}$, for chains of $n = 4$ bonds, for two chain stiffnesses, $\omega = 1.0$ (●) and $\omega = 0.3$ (△). The best-fit curves are simple exponential functions (see text).

and becomes constant for stiffer chains.

4. Averaged Properties of the Interphase

When averaged over the complete interphase, some of the foregoing properties may be expressed as explicit functions of the surface density of the chains. One example is the order parameter. To obtain the average order parameter, $\bar{S}$, S_i^* is summed over bond index i:

$$\bar{S} = n^{-1}\sum_{i=1}^{n} S_i^*$$

In Figure 10, $\bar{S}$ is plotted as a function of $\tilde{A} = \sigma^{-1}$ for $n = 4$, $\omega = \omega_h = 1.0, 0.3$. In that figure, the empirical curve drawn through the calculated points is of the form

$$\bar{S}(\tilde{A}) = (1 - \bar{S}_{dil})e^{-k_s(\tilde{A}-1)} + \bar{S}_{dil} \quad (1)$$

where $\bar{S}_{dil}$ and k_s depend on ω ($\bar{S}_{dil} = -0.114$ and 0.018 for $\omega = 1.0$ and 0.3, respectively) and are not strongly dependent on n ($k_s = 1.9$ and 1.8 for $n = 4$ and 10, respectively; $\omega = 1$). We have determined empirically that $k_s(\omega) \simeq a\omega^{-1} + b$ (a best fit for $n = 4$ gives $k_s(\omega) = 0.183\omega^{-0.988} + 1.74$). These expressions are remarkably accurate representations of the theoretical predictions of $\bar{S}$ for all $\tilde{A}$ and ω. The configurational free energy follows a similar exponential dependence on $\tilde{A}$. For $\omega = 1$ ($k_s = 1.9$), this exponential expression agrees to within 1% with eq A.5 of ref 1, derived through simplifying approximations of the theory.

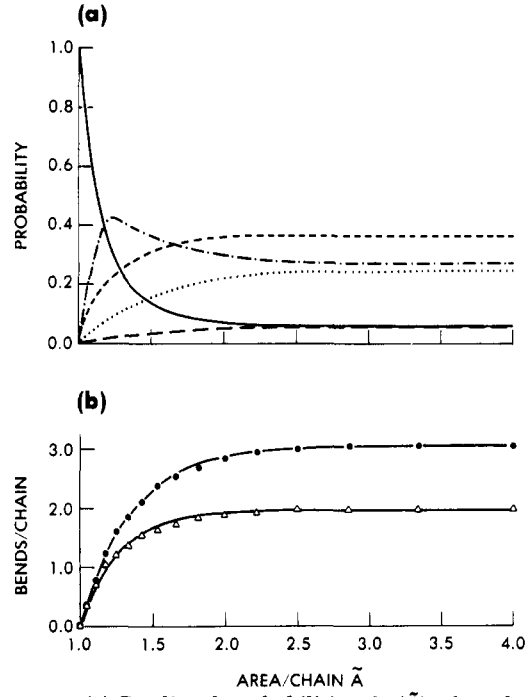

Figure 11. (a) Predicted probabilities, $b_m(\tilde{A})$, that chains of surface density $\tilde{A}^{-1}$ have m total bends; for $n = 4$, $\omega = \omega_h = 0.3$, for $m = 0$ (—), $m = 1$ (-·-), $m = 2$ (- - -), $m = 3$ (···), and $m = 4$ (— — —). (b) Predicted average number of bends/chain for $n = 4$, $\omega = \omega_h$, for chain stiffness $\omega = 1.0$ (●) and 0.3 (△).

The chain-averaged lateral bond probability, $\bar{q}$, can similarly be expressed as an exponential function of $\tilde{A}$ through use of the relations

$$\bar{q} = (n\omega J_1)^{-1}\sum_{j=1}^{n} R_j = (2/3)(1 - \bar{S})$$

(see eq 3.13 and 3.14 of ref 1), where $\bar{S}$ is given by eq 1 above.

The probability, $b_m(\tilde{A})$, that a chain has m total bent bond pairs is shown in Figure 11a (for $n = 4$, $\omega = \omega_h = 0.3$). In the crystalline state ($\tilde{A} = 1$), there can be no bends ($b_0(1) = 1$), but the number of bends increases markedly as $\tilde{A}$ increases. The average number of bends per chain is

$$\bar{b}(\tilde{A}) = \sum_{m=1}^{n} m b_m(\tilde{A})$$

$\bar{b}(\tilde{A})$ is plotted in Figure 11b. This bend probability, as with the average order parameter, is given approximately as an exponential function of $\tilde{A}$:

$$\bar{b}(A) = \bar{b}_{dil}[1 - e^{-k_b(\tilde{A}-1)}]$$

where k_b and $\bar{b}_{dil}$ depend largely on ω; for $n = 4$, $\bar{b}_{dil} = 3.06$ and 1.98 for $\omega = 1.0$ and 0.3, respectively, and $k_b \simeq 1.5k_s$ for both values of ω.

Acknowledgment. This work was supported in part by a National Institutes of Health postdoctoral grant to R.C., No. 1F32 GM09036, and by the Department of Chemistry, University of Florida, Gainesville.

References and Notes

(1) Dill, K. A.; Cantor, R. S. *Macromolecules*, preceding paper in this issue.

(2) Zaccai, G.; Büldt, G.; Seelig, A.; Seelig, J. *J. Mol. Biol.* **1979**, *134*, 693.
(3) Tardieu, A.; Luzzati, V.; Reman, F. C. *J. Mol. Biol.* **1973**, *75*, 711.
(4) Dill, K. A.; Flory, P. J. *Proc. Natl. Acad. Sci. U.S.A.* **1980**, *77*, 3115.
(5) McConnell, H. M. In "Spin Labelling"; Berliner, L. J., Ed.; Academic Press: New York, 1976; p 525.
(6) Charvolin, J.; Manneville, P.; Deloche, B. *Chem. Phys. Lett.* **1973**, *23*, 345.
(7) Mely, B.; Charvolin, J.; Keller, P. *Chem. Phys. Lipids* **1975**, *15*, 161.
(8) Seelig, A.; Seelig, J. *Biochemistry* **1974**, *13*, 4839.
(9) Stockton, G. W.; Johnson, K. G.; Butler, K. W.; Tulloch, A. P.; Boulanger, Y.; Smith, I. C. P.; Davis, J. H.; Bloom, M. *Nature (London)* **1977**, *269*, 267.

Statistical Mechanical Theory of Semidilute Polymer Solutions†

Harumitsu Miyakawa,‡ Keiji Moro, and Nobuhiko Saitô*

Department of Applied Physics, Waseda University, 3-4-1 Okubo, Shinjuku-ku, Tokyo 160, Japan. *Received April 9, 1983*

ABSTRACT: Semidilute poor solvent polymer solution is investigated by the method of Ursell–Mayer cluster expansion. Series and ring-form diagrams are considered for polymers to calculate the osmotic equation of state of the solution, and this equation is shown to be the same as obtained by Edwards by a different method. The static structure factor, which is the Fourier transform of the correlation function of the system, is also calculated in the same approximation; the first term of this factor corresponds to the Jannink–de Gennes result by the random phase approximation. The osmotic compressibility equation, which connects the osmotic pressure and the correlation function, is considered to check the consistency of our results and confirm the validity of the present approximation. Effects of the excluded volume on the equation of state and on the structure factor are investigated up to the first order of the excluded volume parameter z. It is shown that the excluded volume does not affect the osmotic equation of state as well as the structure factor in this approximation.

I. Introduction

We study the semidilute poor solvent polymer solutions based upon the virial expansion theory.[1-3] The semidilute region of polymer solution is defined by Edwards[4] as

$$nv \ll \frac{V}{N} < \kappa_0^{-3} < (nb^2)^{3/2} \tag{I.1}$$

where n is the number of monomer units in a polymer, b is the bond length, N is the number of polymers in solution, V is the volume of the system, v is the excluded volume defined for binary interaction between monomer pairs, and κ_0 is the inverse of the screening length defined by

$$\kappa_0 = \left(\frac{12nvN}{b^2V}\right)^{1/2} \tag{I.2}$$

The region defined by eq I.1 is the same as the semidilute tricritical region (region III in their paper) defined by Daoud and Jannink.[5] In this region, we do not have to rely on the renormalization group (RG) calculations based on the field-theoretic formalism, which is very useful in the theory of good solvent solutions.

The osmotic equation of state in this region was first obtained by Edwards;[4] the equation includes the "Debye–Hückel" term, which represents the fact that the interactions between polymers are screened by the existence of other polymers. Nevertheless, this equation differs completely from that derived by Daoud and Jannink[5] by means of scaling arguments. Moore[6] pointed out this discrepancy and explained that the expression given by Edwards is valid provided that the ternary cluster integral is very small. Furthermore, in the case when the ternary cluster integral (v_2) was assumed to be neglected, Moore obtained the Edwards' "Debye–Hückel" term as a correction to the virial expansion of the osmotic pressure by means of the RG calculation.

In section II, the Saitô theory for solutions, developed by using "grand" canonical ensemble, is first outlined; then it is shown, in the same case where $v_2 = 0$, that this osmotic equation of state is also obtained by summing series and ring-form diagrams, each of which has a single intermolecular interaction between two polymers (see Figure 1) in the formalism of grand partition function.

In the present paper the effect of the ternary interactions, which becomes important to investigate solution properties of polymers at Θ-temperature, is neglected. The effect of these three-body terms on the solution properties of semidilute polymer solution will be discussed in our forthcoming paper.

The structure factor for semidilute polymer solution was first obtained by Jannink and de Gennes[7] using a random phase approximation (RPA), and it was compared with experiments after certain renormalization in small-angle neutron scattering (SANS) by Daoud et al.[8] and in small-angle X-ray scattering (SAXS) by Okano et al.[9] In section III, we calculate the structure factor of the solution by summing diagrams like those given in Figure 1 and show that when the contribution from the ring-form diagrams (Figure 1b) to the structure factor is small compared with that from the series diagrams (Figure 1a) we have the Jannink–de Gennes result.[7]

Recently, des Cloizeaux[10] presented a systematic way to calculate the osmotic pressure and the density correlation function of the semidilute poor solvent solution following grand canonical ensemble formalism in polydisperse systems. The basic idea of his paper is similar to ours and his result for the osmotic pressure including the effect of one-loop diagrams corresponds to Moore's results and ours; moreover, the density correlation function that des Cloizeaux obtained corresponds to the first term of our correlation function, which is given by taking ac-

† Work supported by Grants-in-Aid from the Ministry of Education of Japan.
‡ Deceased.

0024-9297/84/2217-0388$01.50/0